Effects of Metal Ligation and Oxygen on the Reversibility of the Thermal Denaturation of *Pseudomonas aeruginosa* Azurin†

Anders Sandberg,‡ Johan Leckner,§,|| Ying Shi,⊥,# Frederick P. Schwarz,*,⊥ and B. Göran Karlsson*,§

Department of Chemistry, Biochemistry and Biophysics, Göteborg University, and Department of Molecular Biotechnology, Chalmers University of Technology, Box 462, SE-405 30 Göteborg, Sweden, and Center for Advanced Research in Biotechnology/NIST, 9600 Gudelsky Drive, Rockville, Maryland 20850

Received September 10, 2001; Revised Manuscript Received November 19, 2001

ABSTRACT: Thermodynamic equilibrium transition models in DSC are only applicable to reversible processes, but reversibility of the thermal transitions of proteins is comparatively rare because of intermolecular aggregation of denatured proteins and the degradation that occurs at high temperatures. The cupredoxin azurin from *Pseudomonas aeruginosa* has previously been found to exhibit irreversible thermal denaturation, both as holo- and apoprotein [Engeseth, H. R., and McMillin, D. R. (1986) *Biochemistry 25*, 2448−2455]. In this study, however, we demonstrate that this β-barrel protein of Greek key topology in fact unfolds reversibly in anaerobic solutions when nonreducible metal ions are ligated to the protein. We show that it is the metal-coordinating cysteine residue (C112) that becomes exclusively oxidized in a transition metal catalyzed oxidation reaction with dissolved O_2 at high temperatures. Both Cu(I)- and Zn(II)-coordinating wild-type azurin therefore unfold reversibly in anaerobic solutions, as well as the Zn(II)-coordinating disulfide-deficient C3A/C26A mutant. Correspondingly, apoazurin mutants C112A and C112S unfold reversibly, even in aerobic solutions, and exhibit nearly perfect two-state transitions. Unfolding of Cu(II)-coordinating azurin is, on the other hand, always irreversible due to autoxidation of the thiolate resulting in Cu(I) and a thiyl radical prone to oxidation.

Because of the inherent complexity of protein folding, the conformational stability of proteins can at the present time only be determined experimentally. One way to investigate the stability of proteins is in terms of its temperature dependence by differential scanning calorimetry (DSC).[1] In DSC, the thermal denaturation of proteins is monitored by determining the large heat capacity changes accompanying exposure of buried hydrophobic residues upon unfolding of the polypeptide chain. If the thermal transition is reversible, then thermodynamic equilibrium transition models can be applied to the analysis of these transitions to determine a transition temperature (T_m) and a transition enthalpy ($\Delta_{trs}H$). However, for many proteins, thermal denaturation is irreversible mainly due to the slow kinetic process of intermolecular aggregation at temperatures above T_m and the degradative covalent reactions occurring at high temperatures (*1*−*3*), as illustrated by the scheme (*4*):

$$N \leftrightarrow U \rightarrow D \quad (1)$$

where N is the native protein, U is the reversibly unfolded protein, and D is the irreversibly denatured protein. This irreversibility obscures the thermal denaturation by its dependence on the heating scan rate. To resolve the thermodynamics of the unfolding transition from the energetics involved in the slower kinetic processes, it is therefore first necessary to determine the scan rate dependence of the heat capacity changes. Then these changes are extrapolated to infinite scan rate, where it is assumed that the heat capacity changes are the result of the rapid unfolding transition alone (*3*).

Pseudomonas aeruginosa azurin (Figure 1) is a 14 kDa copper-binding protein with an eight-stranded Greek key topology belonging to the cupredoxin family. It has previously been demonstrated that azurin coordinating Cu(II), Zn(II), Hg(II), Ni(II), Cd(II), Ag(I), or Co(II), as well as the apo form, unfolds irreversibly in DSC (*5*). Because the temperature and heat capacity changes accompanying the thermal denaturation of Cu(II) wild-type azurin exhibit a significant scan rate dependence, a T_m of 86.3 °C and a $\Delta_{trs}H$ of 625 ± 73kJ mol^{-1} was later determined by extrapolating to infinite scan rate (*6*). A similar approach has been applied to the closely related cupredoxin plastocyanin, also found to unfold irreversibly, albeit at temperatures approaching 70 °C (*7*). Data have also been reported for the irreversible

† This work has been supported by grants from the Swedish Natural Science Research Council, the Foundation Lars Hiertas Minne, and the Magn. Bergvall Foundation. A.S. acknowledges a grant from the Sven and Lilly Lawski Foundation.

* To whom correspondence should be addressed. F.P.S.: fax, +1 301 738 6255; e-mail, fred@carb.nist.gov. B.G.K.: fax, +46 31 773 3910; e-mail, goran.karlsson@molbiotech.chalmers.se.

‡ Göteborg University.

§ Chalmers University of Technology.

|| Current address: Unité de Bioinformatique Structurale, Institut Pasteur, 25-28 Rue du Docteur Roux, F-75724 Paris Cedex 15, France.

⊥ Center for Advanced Research in Biotechnology/NIST.

Current address: Building 10/9N108, NIDDK, NIH, Bethesda, MD 20892.

[1] Abbreviations: DSC, differential scanning calorimetry; ESI MS, electrospray ionization mass spectrometry; NMR, nuclear magnetic resonance; ESR, electron spin resonance; NOESY, nuclear Overhauser enhancement spectroscopy; GuHCl, guanidine hydrochloride; TMS, sodium 3-(trimethylsilyl)propanesulfonate.

10.1021/bi0157621 CCC: $22.00
Published on Web 12/22/2001

FIGURE 1: Structure of azurin showing the metal site and the three main ligands, His46, Cys112 and His117, in the northern part of the molecule. The disulfide bond between β-strands 1 and 3 is also shown. The strand order in azurin resembles the Greek key motif.

thermal denaturation of the disulfide-deficient Cu(II)-loaded azurin mutant C3A/C26A, which exhibits a significant reduction in conformational stability indicated by an extrapolated T_m of 64.72 ± 0.06 °C and a $\Delta_{trs}H$ of 444 ± 18 kJ mol^{-1} (*8*).

The nature of the thermally induced irreversibility exhibited by both azurin and plastocyanin has, however, not been investigated further. Although the forces behind the conformational stability of proteins are universal, particular amino acids may be critical for the thermal stability in any given case. Thiols are especially vulnerable toward oxidative damage (*9*). Cysteines can react spontaneously with O_2 to form disulfides and sulfenic acid (RSOH) in a reaction catalyzed by transition metals (*10*, *11*), sometimes leading to protein inactivation (*12*, *13*). It has been demonstrated that the main source of irreversibility at elevated temperatures is a combination of the covalent modification of asparagine deamidation (*14*) and the destruction by a β-elimination reaction of cystines and cysteines accompanied by thiol-catalyzed disulfide interchange and formation of sulfenic acid (*14*−*16*). In keeping with the foregoing, many groups have successfully attempted to increase thermal reversibility by mutagenic replacement of free cysteines, e.g., in the case of T4 lysozyme (*17*), both human and bovine Cu,Zn-superoxide dismutases (*18*, *19*), and $\beta\gamma$-crystallin (*20*).

Investigating the nature of the irreversibility of azurin is particularly intriguing, because redox-active metals are known to catalyze the irreversible oxidation of many proteins via a free radical mechanism (*21*). *P. aeruginosa* azurin binds copper by virtue of a type 1 coordination site, i.e., in a distorted trigonal plane formed by a cysteine S^{γ} atom (C112) and two histidine N^{δ} atoms (H46 and H117). In addition, there are two weak axial ligands comprising a methionine S^{δ} atom (M121) and a backbone carbonyl O atom (G45). Since Cu(I) is known to remain associated to C112 in the GuHCl-induced denatured state at room temperature (*22*), a finding which is probably true for most other metal ions as well, there are no free cysteines. Nevertheless, coordination of Cu(II) to azurin still renders its chemical denaturation irreversible (*23*, *24*). This irreversibility is most likely due to a slow copper-catalyzed autoxidation of the thiolate in the denatured state, in accordance with the literature (*25*, *26*). This also explains why other holo forms of azurin, i.e., Zn(II) and Cu(I) coordinated, are highly reversible when chemically denatured at room temperature (*23*, *24*). However, all forms of azurin examined thus far have exhibited irreversible thermal denaturation (*5*, *6*, *8*). Although, e.g., Zn(II) is a redox inactive metal ion, coordination of this ion to the thiolate will increase the electrophilicity of the sulfur atom, rendering it more susceptible to nucleophilic attack by O_2 at high temperatures. Cu(I) is predicted to have the same effect, as well as being able to catalyze the reduction of O_2, yielding reactive radical species by way of the Haber−Weiss cycle (*27*):

$$Cu^{+} + O_2 \rightarrow Cu^{2+} + O_2^{-} \quad (2)$$

$$2O_2^{-} + 2H^{+} \rightarrow H_2O_2 + O_2 \quad (3)$$

$$Cu^{+} + H_2O_2 \rightarrow Cu^{2+} + HO\cdot + HO^{-} \quad (4)$$

Reaction 4 is the copper-catalyzed Fenton reaction. The highly reactive nature of the hydroxyl radical produced during superoxide-driven Fenton chemistry usually results in irreversible covalent modification of a particular amino acid in the immediate vicinity of the metal species (*28*−*30*).

The above reasoning regarding the sensitivity of cysteine toward thermal and metal-catalyzed oxidation prompted us to investigate further the influence of metal coordination and molecular oxygen on the thermal denaturation of *P. aeruginosa* azurin. In this study we demonstrate by means of DSC, electrospray ionization mass spectrometry (ESI MS), nuclear magnetic resonance (NMR) spectroscopy, and electron spin resonance (ESR) spectroscopy the unique role of the metal-coordinating C112 residue in inducing irreversibility of the thermal unfolding transitions of azurin. We show that denaturation of Cu(II)-coordinated wild-type azurin is always irreversible due to autoxidation of the C112 thiolate in the denatured state, but removing molecular oxygen renders the thermal denaturation of Cu(I)- and Zn(II)-coordinating azurin species reversible. In addition, mutagenic replacement of the oxidation-labile cysteine for alanine or serine not only abolishes metal binding but also makes the thermal transitions reversible even in the presence of oxygen. The results presented here indicate that removal of oxygen in DSC might be employed instead of mutagenesis of cysteines or inclusion of DTT to keep cysteines reduced. This would also inhibit the transition metal catalyzed formation of superoxide, and perhaps even hydroxyl radicals, capable of causing irreversible damage to transition metal-coordinating proteins in the denatured state.

EXPERIMENTAL PROCEDURES

Materials. All stock chemicals were reagent grade from Merck.[2] Platinum black was from Fluka. Deionized H_2O was used in all measurements, except in DSC where MQ-H_2O was used.

Mutagenesis, Expression, and Purification of Azurin. The C112A and C112S mutants were constructed using the QuikChange kit (Stratagene) and confirmed by sequencing. Disulfide-deficient C3A/C26A azurin has been described previously (*31*). Mutants and wild-type azurin were expressed and purified as previously described (*32*). The cultivation media used for expression of zinc-loaded derivatives were made 100 μM $ZnSO_4$. The absorption A_{628}/A_{280} ratios were 0.52 for fully oxidized Cu(II)-coordinating wild-type azurin and 0.04 for the Zn(II)-loaded C3A/C26A mutant. C112A, C112S, and Zn(II)-loaded wild-type azurin species exhibited no 628 nm absorption peak after attempting to fully oxidize putative Cu(I) species, indicating the complete absence of copper.

Sample Preparation. All metal-containing azurin samples to be used in NMR and DSC were deoxygenated with concomitant reduction of Cu(II) to Cu(I) using a few grains of platinum black and bubbling of H_2 gas in septum-sealed containers for approximately 30 min. Reduction of Cu(II) to Cu(I) was completely reversible as indicated by full restoration of the A_{628}/A_{280} absorption ratio after bubbling of atmospheric O_2 through the same Pt-containing samples. All samples were kept in these air-tight containers until use. The transfer of samples to the N_2-purged calorimeter was done with syringes through the septum to minimize O_2 contamination. NMR samples were transferred to the restricted NMR tubes under N_2 atmosphere and sealed.

Anaerobic Cu(II) wild-type azurin samples for ESR spectroscopy and ESI MS were deoxygenated by bubbling N_2 gas through the samples for approximately 30 min, after which they were transferred to ESR tubes under N_2 atmosphere and sealed with a rubber cap. Cu(I) wild-type samples to be used in ESR spectroscopy and ESI MS analysis were reduced with Pt and H_2 as described above. Half of the reduced Cu(I) samples were removed from the Pt-containing vessel and purged with atmospheric O_2. Reference solutions were immediately flash frozen in liquid N_2, while the other samples were similarly frozen following thermal denaturation.

ESR Measurements. Cu(II) and Cu(I) wild-type azurin samples were 0.1 mM in 10 mM potassium phosphate buffer, pH 7.0. Half of each prepared sample was removed and flash frozen in liquid N_2 as reference. Remaining solutions were denatured at 95 °C for 5 min and allowed to cool to room temperature for 5 min prior to being frozen in liquid N_2. ESR measurements were performed on a Bruker ESP 300 E spectrometer with a Bruker X-band ESP 380-1010 microwave bridge at 77 K. Microwave frequency and power were 9.27 GHz and 2 mW, respectively. Modulation amplitude was 20 G, and modulation frequency was 100 kHz.

ESI MS Measurements. Samples were 0.1 mM in 10 mM potassium phosphate buffer, pH 7.0, when thermally denatured. All samples were treated as described above with regard to ESR spectroscopic measurements. Liquid chromatography/MS was performed using a short column, 50 × 1 mm, packed with ACE C_8 3 μm particles (300 Å) (Hichrom) in isocratic mode with 65% acetonitrile containing 0.05% formic acid as the mobile phase. An HP 1100 series binary pump (Hewlett-Packard) was used, delivering 0.2 mL/min, and the flow was split down to 65 μL/min by a Valco T with 40 cm of a 50 μm fused silica restrictor before the column. The sample (1 μL) was injected using a Rheodyne 7520 injector. Electrospray mass spectra were acquired on a Q-Tof mass spectrometer (Micromass) operating in the positive ion mode with a Z-spray electrospray ion source. Dry nitrogen was used as nebulizing and desolvation gas (300 L/h) with a desolvation temperature of 300 °C and the sample cone at 100 °C. The electrospray probe was kept at +3 kV.

Absorbance Measurements. The T_m and van't Hoff enthalpy (ΔH_{vH}) of apoazurin C112A and C112S, and the T_m of Zn(II) C3A/C26A, were estimated using a Cary 4 UV/vis spectrophotometer calibrated with a digital thermometer inserted in the cuvette. The scan rate was 0.3 °C/min, ranging from 30 to 90 °C. The A_{280}/A_{291} absorption ratio was plotted against T, and data were analyzed according to ref *33* using the Igor Pro program (Wavemetrics). The uncertainties are a combination of those of the curve-fitting procedure and imprecision in temperature readings. Absorption spectra from 310 to 240 nm were recorded before and after the denaturation to validate the structural integrity of the protein, with emphasis on the characteristic azurin W48 absorption peak at 291 nm. Concentrations were 0.1 mM azurin in 10 mM potassium phosphate buffer, pH 7.0.

NMR Measurements. Azurin used for the NMR measurements were 1 mM in 10 mM potassium phosphate buffer, pH 5.5. Buffer was made 10% D_2O in one set of experiments, in which the samples were thermally denatured in the NMR tubes by submerging them in 95 °C H_2O for 5 min. 1D spectra were recorded with 128 transients, 16K points, and a sweep width of 8000 Hz. 2D NOESY spectra were recorded with 32 transients, 256 increments, 2K points, and a sweep width of 7000 Hz. This set of experiments was recorded at 30 °C on a 500 MHz Varian INOVA spectrometer. In another set of experiments, buffer was made >95% D_2O, and TMS [sodium 3-(trimethylsilyl)propanesulfonate] was added as a reference. These samples were subjected to a gradual temperature increase of 5 °C per step. After an equilibration period at each temperature for at least 15 min, a 1D spectrum was recorded with 64 transients, 4K points, and a sweep width of 7000 Hz. The high-temperature spectra were run on a 500 MHz Varian Unity Plus spectrometer.

DSC Measurements and Analysis. DSC measurements were performed using a VP-DSC microcalorimeter (Microcal, Inc.). The DSC consists of a matched pair of 0.511 mL sample and reference cells. Both cells were first loaded with buffer solution, equilibrated at 288 K for 15 min, and typically scanned from 15 to 105 °C at a scan rate of 40−80 K h^{-1}. The buffer versus buffer scan was repeated once, and upon the second cooling, the sample cell was emptied, rinsed, and loaded with the protein solution prior to the 15 min equilibration period. This procedure was repeated for

[2] Certain commercial equipment, instruments, and materials are identified in this paper in order to specify the experimental procedure as completely as possible. In no case does this identification imply a recommendation or endorsement by the National Institute of Standards and Technology, nor does it imply that the material, instrument, or equipment identified is necessarily the best available for the purpose.

Table 1: Thermodynamic Parameters of the Thermal Unfolding of Metal Derivatives of Wild-Type Azurin and the Zn(II) C3A/C26A Azurin Mutant

azurin derivative	scan rate (K h^{-1})	concn (mM)	T_m (°C)	$\Delta_{trs}H$ (kJ mol^{-1})	$\Delta_{trs}H_{vH}$ (kJ mol^{-1})	$\Delta_{trs}H_{vH}/\Delta_{trs}H$
Zn(II) C3A/C26A	80	0.059	72.4 ± 0.1	459 ± 19	552 ± 17	1.20 ± 0.06
second scan			72.9 ± 0.1		560 ± 17	
Zn(II) C3A/C26A	40	0.059	72.0 ± 0.1	473 ± 20	567 ± 17	1.15 ± 0.06
second scan			72.3 ± 0.1		590 ± 18	
Cu(II) C3A/C26A[a]			62.72 ± 0.06	444 ± 18		1.00
Zn(II) wild type	80	0.083	89.6 ± 0.1	660 ± 28	765 ± 23	1.16 ± 0.06
second scan			89.8 ± 0.1		786 ± 24	
Zn(II) wild type	40	0.083	89.0 ± 0.1	688 ± 29	795 ± 24	1.16 ± 0.06
second scan			89.0 ± 0.1		810 ± 34	
Cu(I) wild type	80	0.06−0.088	85.4 ± 0.5	467 ± 20	590 ± 63	1.26 ± 0.23
second scan			86.4 ± 0.6		556 ± 28	
Cu(I) wild type	40	0.088	83.7 ± 0.1	524 ± 22	733 ± 21	1.40 ± 0.06
second scan			84.7 ± 0.1		680 ± 20	
Cu(II) wild type[b]			86.3	625 ± 73		1.00

[a] From ref *8*. [b] From ref *6*. These are extrapolated values to infinite scan rate.

Table 2: Thermodynamic Parameters of the Thermal Unfolding of the Cysteine Azurin Mutants

azurin mutant	scan rate (K h^{-1})	concn (mM)	pH	T_m (°C)	$\Delta_{trs}H$ (kJ mol^{-1})	$\Delta_{trs}H_{vH}$ (kJ mol^{-1})	$\Delta_{trs}H_{vH}/\Delta_{trs}H$
C112S	80	0.061	7.0	65.7 ± 0.1	515 ± 22	470 ± 14	0.91 ± 0.05
second scan				65.7 ± 0.1		559 ± 17	
C112S	60	0.090	7.0	65.3 ± 0.1	526 ± 22	518 ± 15	0.98 ± 0.05
C112S		0.076	6.5	66.9 ± 0.1	514 ± 22	535 ± 15	1.04 ± 0.05
C112S		0.029	6.3	68.9 ± 0.1	575 ± 40	573 ± 17	1.00 ± 0.07
C112S		0.011	5.9	69.3 ± 0.1	565 ± 28	564 ± 17	1.00 ± 0.06
C112A	80	0.056	7.0	59.6 ± 0.1	303 ± 15	374 ± 11	1.23 ± 0.07
second scan				59.8 ± 0.1		325 ± 10	
C112A	60	0.028	7.0	59.9 ± 0.1	299 ± 12	290 ± 10	0.97 ± 0.05
C112A		0.057	6.5	61.2 ± 0.1	312 ± 19	382 ± 11	1.22 ± 0.06
C112A		0.026	6.2	64.0 ± 0.1	367 ± 17	359 ± 11	0.98 ± 0.05

the other protein solutions after each solution sample was scanned twice to check for repeatability of the transition. The sample solutions were from 0.02 to 0.05 mM in 10 mM potassium phosphate buffer, with pH ranging from 5.9 to 7.0 (cf. Tables 1 and 2). For the scans run under oxygen-free conditions, the solution from the previous scan was removed, and the sample cell was washed with buffer and then purged with dry N_2 prior to injection of the next sample solution. The data were recorded every 10 s. After completion of a series of DSC scans, the second buffer versus buffer scan was used as the baseline scan and subtracted from the protein scans prior to analysis. The net DSC scan was analyzed for thermodynamic parameters by using the EXAM software program (*34*). The pre- and posttransitional baselines were determined from least-squares fits of straight lines to the data points, respectively, below the onset of the transition peak and following the return of the transition peak to the baseline. A sigmoidal baseline was determined under the transition peak by extrapolating the pre- and posttransitional baselines and employing the profile of the transition peak (*34*). For the transitions, which exhibited repeatability, implying that they were reversible, a two-state A ↔ B transition model was used to obtain the T_m and the van't Hoff enthalpy ($\Delta_{trs}H_{vH}$) for the transition. Values for $\Delta_{trs}H$ were determined from the ratio of the transition peak area to the number of moles of protein in the sample vessel. For the nonrepeatable transitions exhibiting scan rate dependence, just the area and temperatures at the peak maximum were recorded.

The standard uncertainty in T_m determined from imprecision in the temperature readings and imprecision in the fractional areas under the transition peak is estimated to be ±0.1 K. The combined estimated uncertainty in the van't Hoff enthalpy from imprecision in the fractional area under the transition peak was estimated to be 3%. The combined estimated uncertainty in $\Delta_{trs}H$ contains uncertainty contributions from the area under the transition peak, the concentration of protein (3%), and the heat calibration of the DSC and is 4.2%. As shown in Tables 1 and 2, the standard deviations of the mean values of $\Delta_{trs}H_{vH}$ and $\Delta_{trs}H$ are close to the combined estimated uncertainties of these values.

RESULTS

ESR Measurements. Figure 2 shows the ESR spectra of anaerobic and aerobic Cu(II) and Cu(I) wild-type azurin samples before and after thermal denaturation at 95 °C for 5 min. Paramagnetic Cu(II) ion coordinated to azurin gives spectra with narrow hyperfine splittings characteristic of azurin (Figure 2a,b, broken lines). Upon thermal denaturation in the absence of oxygen the signal is reduced considerably (Figure 2a, solid line), consistent with autoxidation of the thiolate resulting in a diamagnetic Cu(I) ion. Interestingly, the shape of the remaining signal, amplified 10× in Figure 2a, indicates a strong Cu(II) complex based on its resemblance to a simulated ESR spectrum with an $A_{||}$ of 209 and a $g_{||}$ of 2.134 (not shown). In the presence of dissolved O_2, however, Cu(I) becomes reoxidized, resulting in an ESR spectrum resembling that of a Cu(II) complex previously

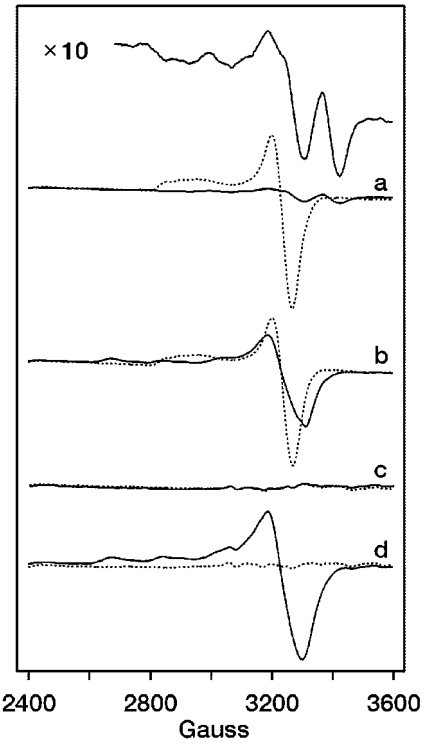

FIGURE 2: ESR spectra of (a) anaerobic Cu(II) with an amplified postdenaturation signal, (b) aerobic Cu(II), (c) anaerobic Cu(I), and (d) aerobic Cu(I) wild-type azurin samples before (broken lines) and after (solid lines) denaturation at 95 °C for 5 min. Samples were 0.1 mM azurin in 10 mM potassium phosphate, pH 7.0.

found for thermally denatured azurin (*35*), reflecting unspecific ligation primarily to nitrogen atoms (Figure 2b, solid line). This reduction of dissolved O_2 to O_2^- by Cu(I) and unspecific ligation of the resulting Cu(II) to denatured protein is also evident in the case of thermal denaturation of Cu(I)-coordinating wild-type azurin (Figure 2d).

ESI MS. Electrospray ionization mass spectrometric analysis of aerated Cu(I)-loaded as well as Cu(II)-loaded wild-type azurin after denaturation in 95 °C for 5 min revealed the presence of a significant population of dimers (Figure 3A,C), semiquantitatively estimated to be around 75% of the total population. The monomeric population observed in both cases was oxidized protein of 13976 Da. Since apo wild-type azurin has a molecular mass of 13945.81 Da, the resulting monomers could correspond to C112 becoming oxidized to form sulfinic acid (RSO_2H). In the case of deaerated Cu(I)-loaded azurin, however, a nonoxidized monomeric population of 13945 Da predominates, with dimeric species being virtually absent (Figure 3D). In contrast, a significant dimeric population was obtained in the anaerobic Cu(II) sample (Figure 3B), estimated to correspond to about 25% of the total amount of species. Observed monomers in this sample were similar to those obtained from anaerobic Cu(I) denaturation, i.e., having a molecular mass equal to apo wild-type azurin. The metal was lost in all measurements, even in reference spectra of nondenatured azurin (not shown).

NMR and Absorbance Measurements. The structural integrities of apo mutants C112A and C112S were examined using NMR techniques. A comparison of the wild-type and mutant 2D NOESY spectra revealed that the structures of both mutant proteins were virtually identical to that of the

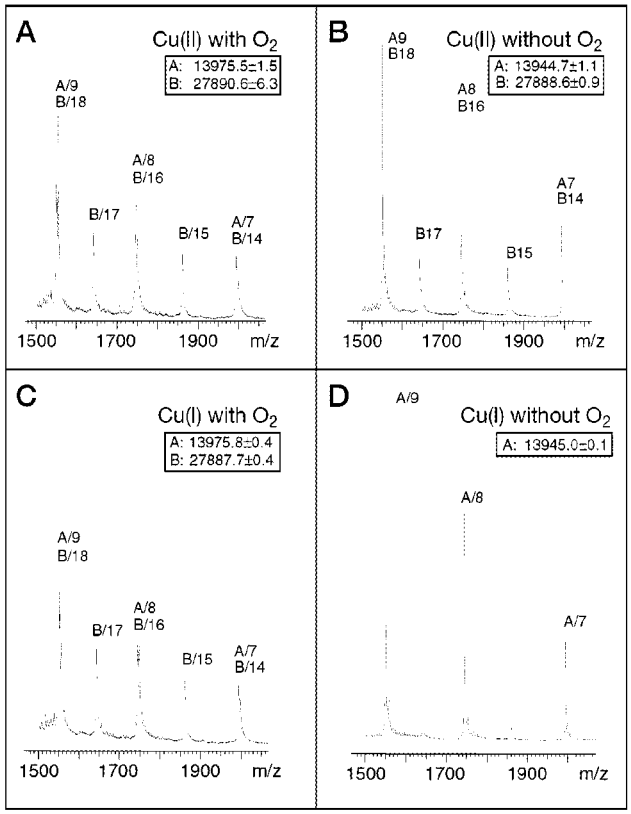

FIGURE 3: Mass spectra of (A) aerobic and (B) anaerobic Cu(II) and (C) aerobic and (D) anaerobic Cu(I)-coordinating wild-type azurin samples after denaturation at 95 °C for 5 min. Samples were 0.1 mM azurin in 10 mM potassium phosphate, pH 7.0.

wild-type protein, except in the immediate vicinity of the mutation (data not shown).

To examine the temperature-dependent behavior of azurin, 2D NOESY spectra of C112A, C112S (aerobic solutions), and zinc-containing C3A/C26A (anaerobic solution) azurin were recorded before and after thermal denaturation at 95 °C for 5 min. The spectra of the heated samples, recorded at 30 °C, were indistinguishable from those recorded before heating of the sample (data not shown). Despite the high protein concentration (1 mM), no precipitate was observed in the NMR tubes in either case.

In aerobic temperature scanning absorbance measurements, the T_m values of the C112A and C112S apo mutants were 59.7 ± 0.5 °C (ΔH_{vH} = 300 ± 4.5 kJ mol^{-1} K^{-1}) and 65.0 ± 0.5 °C (ΔH_{vH} = 512 ± 6.6 kJ mol^{-1} K^{-1}), respectively (Figure 4), and the T_m of the zinc-containing C3A/C26A was found to be 72.9 ± 0.04 °C (data not shown). The heating of the NMR samples at 95 °C for 5 min is therefore expected to denature completely all of the azurin derivatives used in this study, but only an NMR spectrum recorded at a temperature above T_m would confirm the protein to be completely denatured. Technical limitations precluded the recording of a high-resolution 2D spectrum at temperatures above the T_m of the mutants. Instead, temperature titrations of Cu(I) wild-type, Zn(II) C3A/C26A, and C112A azurin were performed in a series of 1D NMR experiments (Figure 5). The experiments were performed in D_2O to facilitate water suppression, and the Cu(I) wild-type and Zn(II) C3A/C26A azurin samples were kept under nitrogen atmosphere. In all three cases, the temperature was raised until the signals originating from the upshifted methyl groups disappeared,

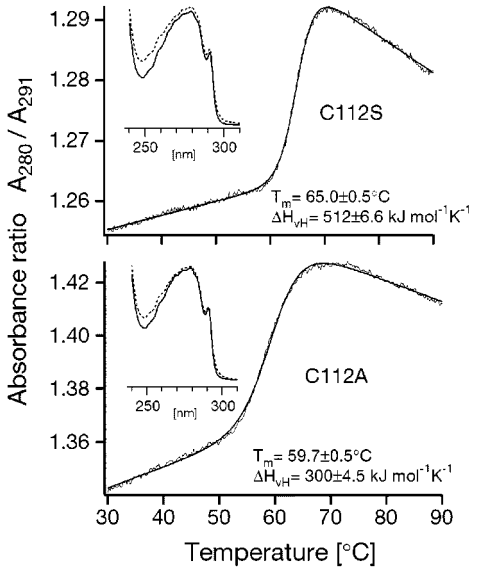

FIGURE 4: Temperature scanning absorbance measurements of 0.1 mM C112A and C112S azurin in 10 mM KP_i, pH 7.0, with curve fit. The scan rate was 0.3 °C/min. Inserted are the electronic spectra before (solid lines) and after (broken lines) thermal denaturation of the same samples.

indicating complete loss of tertiary structure. The exchange of all amide protons for deuterons, as evident in Figure 5, also supports complete unfolding of azurin at temperatures above T_m. To ensure thermal equilibrium, the samples were kept at each temperature for at least 15 min, after which no further changes in the NMR spectra were observed. Consequently, the protein samples were kept at high temperature for a considerable time, and as a result precipitates were eventually formed in the NMR tubes. Formation of precipitate is evident in all three samples as a decrease in signal intensity after denaturation. Precipitate formation is probably a concentration-dependent side reaction in the folding process. Following the NMR-monitored temperature titration, the Cu(I)-coordinating wild-type azurin sample tube was opened, and the precipitate was collected and dissolved in 5 M GuHCl. The protein was brought to conditions favoring the folded state by dilution, and after reoxidation of Cu(I) more than 50% of the protein from the precipitate could be restored into the blue Cu(II) form.

DSC Measurements. Typical DSC scans of the Zn(II)-coordinating C3A/C26A azurin mutant in the presence of air, as shown in Figure 6c, exhibit a dependence of the temperature maximum and of $\Delta_{trs}H$ on scan rate. More specifically, the temperature maximum and enthalpy are respectively 68 ± 0.1 °C and 364 ± 15 kJ mol^{-1} at 40 K h^{-1} and 71 ± 0.1 °C and 394 ± 17 kJ mol^{-1} at 80 K h^{-1}. Furthermore, the transitions do not reappear upon subsequent cooling and heating of the samples (not shown). When scanning from 15 to 105 °C under oxygen-free conditions, however, the transition does reappear upon a rescan of the sample, as shown in Figure 6a, and the transition temperature and enthalpy are independent of scan rate as shown in Table 1. A fit of the two-state transition model to the first scan shown in Figure 6b and to scans at other scan rates yields average values of T_m = 72.2 ± 0.2 °C and $\Delta_{trs}H$ = 466 ± 7 kJ mol^{-1}. The van't Hoff enthalpy, $\Delta_{trs}H_{vH}$, determined from the fit of the two-state transition model to the data, yields an average value of 567 ± 16 kJ mol^{-1} at both scan

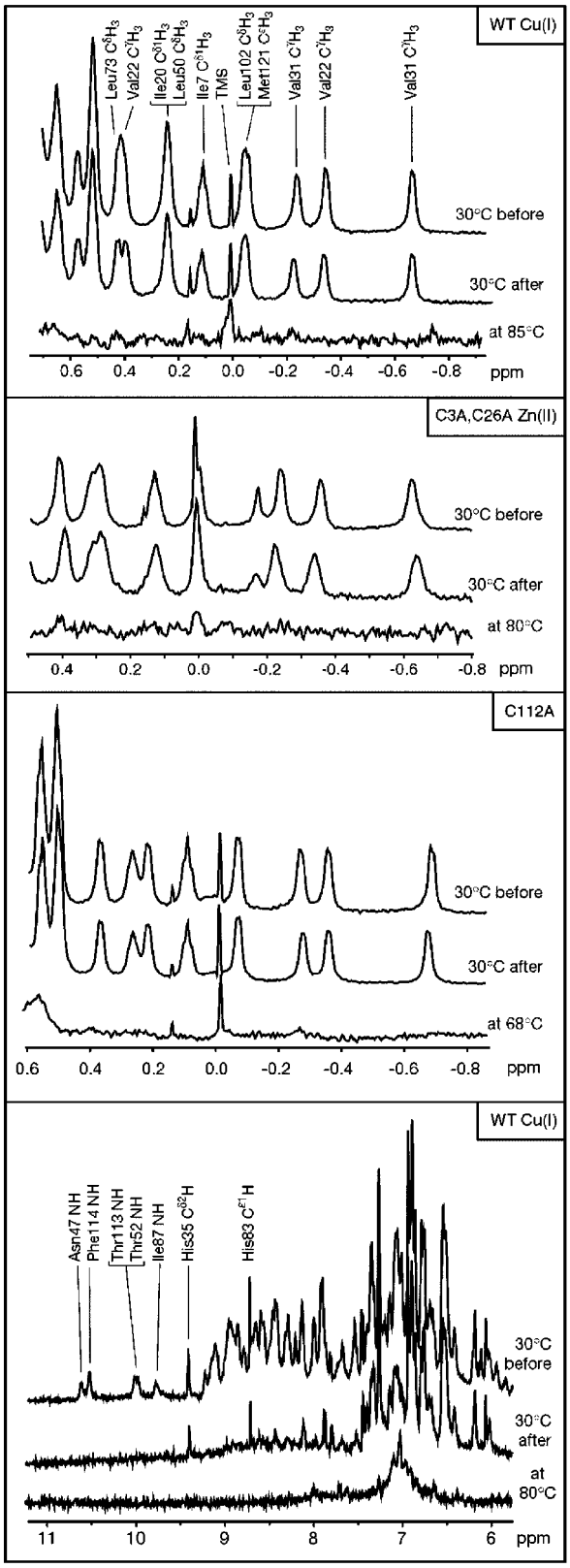

FIGURE 5: 1D NMR temperature titrations of 0.1 mM Cu(I)-loaded wild-type (WT), Zn(II)-loaded C3A/C26A, and apo-C112A azurin. Displayed are the methyl regions, as well as the Cu(I)-coordinating wild-type amide proton region. All samples were >95% D_2O in 10 mM potassium phosphate buffer, pH 5.5.

rates. Application of the transition model to the data from the second scan yielded the same values for T_m and $\Delta_{trs}H_{vH}$ to within the uncertainties as determined from analysis of the first scan transition peak at both scan rates, showing that

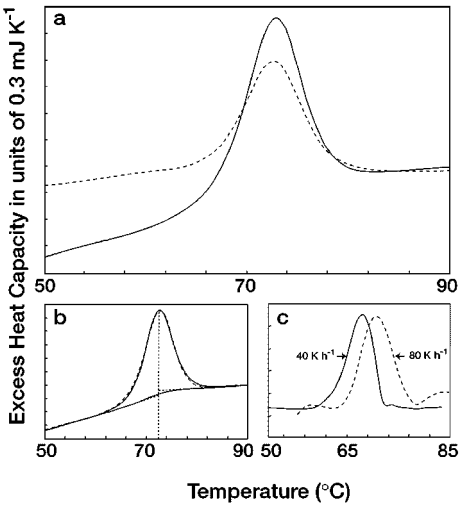

FIGURE 6: (a) DSC scans of deaerated 0.059 mM Zn(II) C3A/C26A azurin in 10 mM potassium phosphate buffer, pH 7.0, at 80 K h^{-1}. This sample was scanned from 15 to 105 °C. The broken line is the repeat scan of the same solution. (b) A fit of the two-state transition model to the deaerated 0.059 mM Zn(II) C3A/C26A azurin mutant thermal transition peak at a scan rate of 40 K h^{-1}. Broken lines are the extrapolated baselines and the transition temperature determined from the fit. (c) Aerated 0.042 mM Zn(II) C3A/C26A azurin in 10 mM potassium phosphate buffer, pH 7.0, at 40 and 80 K h^{-1}. Sample volumes were 0.511 mL.

the transition is reversible. Values for $\Delta_{trs}H$ were less for the second scan of the sample as shown in Figure 6a by the reduced area of the transition peak. These reductions in the transition enthalpy result from some thermal degradation of the protein during prolonged exposure at high temperature during the first scan and, thus, are not presented in Table 1. The transition temperature is higher than the extrapolated value for Cu(II)-coordinating C3A/C26A azurin (*8*), while the transition enthalpy is close to that of the extrapolated value from the literature (*8*) in Table 1.

Similar DSC results were obtained for the Cu(I) and Zn(II) wild-type azurin derivatives scanned under oxygen-free conditions. The DSC scans were repeatable as shown in Figure 7, and the transition temperatures and enthalpies were independent of scan rate as shown in Table 1. A typical fit of the two-state transition model to the Zn(II) azurin transition peak is presented in an insert in Figure 7b. Although the transition and van't Hoff enthalpies are within twice the uncertainties and may be considered the same for the Cu(I) azurin derivative, the transition temperatures are slightly higher at the faster scan rate. It is not known as to why the temperatures are different. The reproducible transition temperatures and enthalpies upon a rescan of the solution indicate that the transition is reversible. Values for $\Delta_{trs}H$ for the second scan in Table 2 are not presented since again the values depend on the scan rate conditions and are reduced as shown in Figure 7. For the Zn(II)-coordinating azurin derivative, prolonged exposure to air resulted in the transition in Figure 7c, which did not reappear upon a rescan of the solution. Thus, in the presence of air and similar to that of the Cu(II) wild-type azurin transition, the transition is irreversible and dependent on scan rate (not shown). As expected, the Zn(II) azurin derivative is slightly more thermally stable, and the Cu(I) azurin derivative is slightly less thermally stable, than Cu(II) azurin (*5*, *6*).

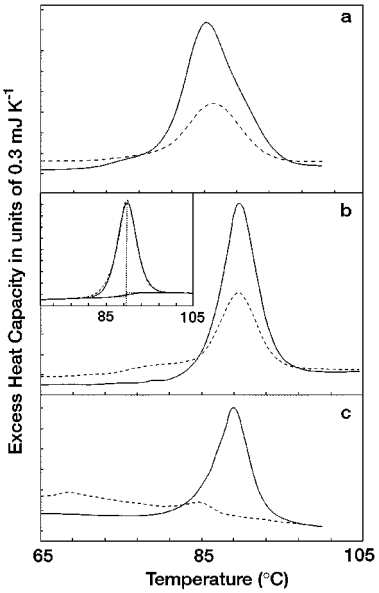

FIGURE 7: (a) DSC scan of deaerated 0.061 mM Cu(I) wild-type azurin in 10 mM potassium phosphate buffer, pH 7.0, at 80 K h^{-1}. The broken line is the repeat scan of the same solution. (b) DSC scan of deaerated 0.044 mM Zn(II) wild-type azurin in 10 mM potassium phosphate buffer, pH 7.0, at 80 K h^{-1}. The broken line is the repeat scan of the same solution. Inserted is the fit of the two-state transition model to the peak of the first scan. The extrapolated baselines and the transition temperature determined from the fit are also shown as broken lines. (c) DSC scan of aerated 0.05 mM Zn(II) wild-type azurin in 10 mM potassium phosphate buffer, pH 7.0, at 40 K h^{-1}. The broken line is the repeat scan of the same solution. Sample volumes were 0.511 mL.

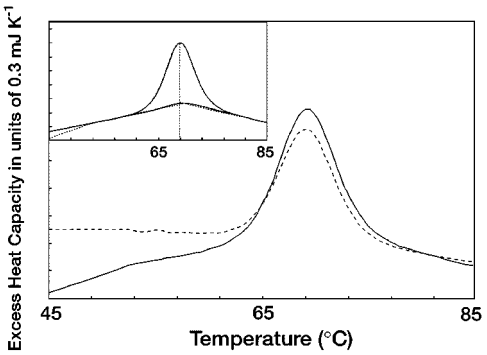

FIGURE 8: DSC scans of the 0.029 mM C112S azurin mutant in 10 mM potassium phosphate buffer, pH 6.3, at 60 K h^{-1}. The broken line is the repeat scan of the same solution. Inserted is the fit of the two-state transition model to the same scan. The broken lines are the extrapolated baselines and the transition temperature determined from the fit. The sample volume was 0.511 mL. Apo mutants were scanned from 15 to 85 °C.

Typical DSC results on the thermal transitions of the apo mutants of azurin are presented in Figure 8 for C112S. Both the C112A and C112S mutants were scanned from 15 to 85 °C, and the transitions did not exhibit scan rate dependence and were repeatable even in the presence of dissolved molecular oxygen. Results of the fit of a two-state transition model to the DSC data, as shown for C112S in Figure 8, are presented in Table 2. Since T_m and $\Delta_{trs}H_{vH}$ are the same upon a rescan of the sample, the transitions are reversible. The transition enthalpies, $\Delta_{trs}H$, for the second scan are not presented since they depend on the amount of protein in the sample, which depends on the upper temperature limit of the first scan and the scan rate due to thermal degradation

of the protein at high temperature. For example, this is shown in Figure 8 by the reduced transition peak area of the second scan for the C112S mutant. The dependence of the transition enthalpy and temperature on pH is also presented in Table 2. These quantities increase with a decrease in pH, which indicates that the unfolded state of the protein is preferentially destabilized by protonation of its residues. Assuming that the dependence of the transition enthalpy is linear with respect to the transition temperature, the transition enthalpy can be extrapolated up to the transition temperature for azurin. An extrapolation of the C112A results, where $d(\Delta_{trs}H)/dT = 15.4 \pm 2.4$ kJ mol^{-1} K^{-1}, up to 86.3 °C, yields a transition enthalpy of 710 ± 54 kJ mol^{-1}, which is close to the extrapolated value of 625 ± 73 kJ mol^{-1} for Cu(II) wild-type azurin from the literature (*6*). Apparently, the copper ion binding enthalpy is close to zero, indicating that metal stabilization is mainly entropic. An extrapolation of the C112S results was not performed because of the large uncertainty in $d(\Delta_{trs}H)/dT = 13.9 \pm 4.4$ kJ mol^{-1} K^{-1}.

DISCUSSION

The ability of redox-active transition metals to oxidize thiols is well-known and has been demonstrated in a number of cases (*26*). We decided to investigate if this mode of protein inactivation is also in effect in the thermal denaturation of the copper-binding protein *P. aeruginosa* azurin, since such a reaction has been implicated from previous chemical denaturation studies (*23*, *24*, *36*). As can be seen from the ESR spectra in Figure 2, denaturation of Cu(II)-coordinating azurin by heating at 95 °C for 5 min gives quite different results for aerobic and anaerobic solutions. Anaerobic denaturation proves that autoxidation of the copper-coordinating thiolate is in effect, since most of the signal is lost following conversion of paramagnetic Cu(II) into diamagnetic Cu(I). The shape of the remaining signal (Figure 2a, solid line) is interesting, however, because its parameters ($g_{||} = 2.134$ and $A_{||} = 209$ G) are indicative of a type 2 copper ion. Thus, it appears that the native geometry around the metal, i.e., type 1 coordination, has been distorted. This, in turn, suggests the presence of an intermediate in the thermal unfolding process, occurring before the redox reaction between Cu(II) and thiolate. An unfolding intermediate has in fact been suggested previously (*35*). Copper complexes with four coordinating nitrogens are known with ESR parameters in this range ($g_{||} = 2.16$ and $A_{||} = 200$ G) (*37*). However, it seems more likely that a sulfur is still coordinated since sulfur ligands are known to reduce the $g_{||}$ value even more (*38*). Furthermore, the line width of the spectrum is smaller than would have been expected with unresolved ligand hyperfine interaction from four ^{14}N nuclei.

In the presence of molecular oxygen, the ESR spectrum of denatured Cu(II) is transformed from that characteristic of a type 1 coordination to one resembling unspecific Cu(II) ligation, resulting from reoxidation by molecular oxygen of the Cu(I) released during the autoxidation reaction. The magnitude of this signal masks the signal of the type 2 intermediate. Similarly, thermal denaturation of diamagnetic Cu(I)-coordinated wild-type azurin results in a paramagnetic Cu(II) signal only in the presence of O_2. This is also consistent with oxidation of Cu(I) to Cu(II) by reduction of molecular oxygen to superoxide, which is known to occur even at room temperature (*27*).

We cannot rule out that a direct attack of molecular oxygen on the thiol occurs faster than the autoxidation reaction, resulting in the same Cu(II) ESR spectra as in Figure 2b. However, we deem this to be unlikely because we ascribe the electron transfer between thiolate and ligand to the exothermic effect observed in previous DSC measurements of Cu(II)-loaded wild-type azurin (*5*, *6*) and plastocyanin (*7*). No such exothermic process is observed when nonreducible metal ions are present in the metal-binding site of *P. aeruginosa* azurin (*5*). In addition, it is also absent in the DSC profile for Cu(II)-loaded C3A/C26A azurin (*8*), which probably reflects the slower nature of the reaction at the lower T_m. Reduction of Cu(II) during autoxidation of cysteine has in fact been suggested to be the rate-limiting reaction, as well as an obligatory intermediate, in the overall process of copper-catalyzed cysteine oxidation at room temperature (*25*), consistent with the slow nature of this reaction observed in chemically denatured azurin (*24*). At the temperature required to denature Cu(II) wild-type azurin, however, we speculate that this reaction will occur rapidly.

Further insight into the irreversibility of the thermal transition was obtained by mass spectrometric analysis of Cu(I)- and Cu(II)-coordinating azurin after heating in the absence and presence of molecular oxygen. Autoxidation of thiolate results in a thiyl radical (RS•) that has a tendency to react with electron-rich centers such as oxygen or to combine with other thiyls to form cystines (*39*). A qualitative difference is in fact observed for anaerobic and aerobic thermal denaturation. As can be seen in Figure 3, in the absence of dissolved O_2 Cu(I) wild-type azurin does not become oxidized and has a molecular mass equal to apo wild-type azurin (13945.81 Da) since the metal is displaced during the mass spectrometric measurements. In the presence of O_2, however, the C112 residue becomes oxidized to form two main populations: dimers (approximately 27889 Da) and oxidized monomers (approximately 13976 Da). The fact that thermally denatured Cu(I)-coordinating azurin gives rise to such a significant proportion of disulfides in the presence of O_2 also indicates that Cu(II) is formed by reduction of molecular oxygen, since only Cu(II) can efficiently catalyze the oxidation of cysteines into cystines. The molecular mass of the monomers corresponds well with oxidation of the C112 thiolate into sulfinic acid (RSO_2H), although oxidation of other residues is also possible as the metal is displaced during oxidation of the thiolate. The irreversibly unfolded disulfide species should therefore in principle be refoldable under reducing conditions, unlike the irreversibly unfolded monomeric population. However, the concomitant reduction of the intrinsic disulfide of azurin would significantly destabilize the folded state. These results offer an explanation of the results previously published for plastocyanin, where two thermally denatured populations were observed: one reversible only with copper and reductant and one irreversible (*40*). Thermally denatured Cu(II)-loaded azurin, on the other hand, does form disulfide-bonded dimers even in the absence of dissolved O_2, as the thiyl radicals produced during autoxidation combine to form cystines. The monomeric population is, of course, not oxidized. In addition, denaturation of Cu(II) azurin in the presence of O_2 gives results comparable to those of aerobically denatured Cu(I) azurin.

Interestingly, observed dimeric species are never oxidized further than to disulfide even in the presence of O_2, indicating

that it is the metal-binding cysteine that becomes exclusively oxidized. In addition, the absence of oxidized monomers other than sulfinic acid in the mass spectra is indicative of three interesting points: (a) The superoxide produced from Cu(I) reduction of O_2 immediately reacts with the thiyl radical, thus producing stable sulfinic acid. Apparently, reaction between O_2 and thiyl does not occur to any significant amount, since this would result in a RSOO$^{\bullet}$ radical species capable of undergoing further oxidation reactions, but this is not observed in any of the mass spectra. (b) It does not appear as if superoxide-driven Fenton chemistry is in effect based on these mass spectrometric results, since this would result in oxidized species other than those observed. (c) We find no evidence of β-elimination reactions of cysteine residues occurring during the 5 min incubation at 95 °C.

The results discussed above prompted us to investigate if nonreducible metal species coordinated to azurin would render the thermal transition reversible in the absence of molecular oxygen. In fact, removal of O_2 as a way of increasing thermal reversibility has previously been implicated for bacteriophage T4 lysozyme (*41*). Anaerobic NMR spectroscopic analysis (Figure 5) and DSC measurements of Cu(I)- and Zn(II)-coordinating azurin (Table 1 and Figure 7) confirmed the involvement of an oxidation step in the irreversible thermal denaturation of this protein, in analogy with what has been suggested previously for the related cupredoxin plastocyanin (*40*).

Since Cu(II) azurin is more resistant toward GuHCl-induced denaturation than Zn(II)- or Cu(I)-loaded forms (*23*, *24*), one would intuitively expect Cu(II) azurin to exhibit higher thermal stability. Considering that the T_m and $\Delta_{trs}H$ are lower for Cu(II) than for Zn(II) or Cu(I) azurin, however, one might suspect that autoxidation of the thiolate actually triggers the unfolding of Cu(II)-coordinating wild type at a certain temperature. Therefore, we also examined the Zn(II)-loaded C3A/C26A azurin mutant with DSC, since this mutant denatures at temperatures around 70 °C. This disulfide-deficient mutant was also found to denature reversibly in the absence of molecular oxygen (Figures 5 and 6), and because the T_m and $\Delta_{trs}H$ for Zn(II) C3A/C26A azurin are higher than those extrapolated for Cu(II) C3A/C26A (cf. Table 1), in analogy with wild-type azurin, we conclude that autoxidation of cysteine in Cu(II)-coordinating wild-type azurin does not trigger the thermal unfolding of this protein. In addition, since the thermal denaturation of the C3A/C26A mutant is irreversible in the presence of O_2, intramolecular disulfide exchange reactions are not the primary cause of irreversibility in azurin. Again, the C112 residue is implicated.

Replacing the metal-coordinating cysteine with serine (C112S) or alanine (C112A) by mutagenesis completely abolishes metal binding in azurin, as has previously been described for the C112S mutant (*42*). 2D NMR NOESY spectra revealed the native structure to be conserved (data not shown), in accordance with published crystal structures for holo- (*43*, *44*) and apoazurin (*45*). Absorbance measurements (Figure 4) and DSC of these apo mutants (Figure 8, Table 2) confirm the remarkable stabilizing role of the metal, believed to be mainly entropic, as well as finally proving that C112 is oxidation-labile and the main cause of thermal irreversibility. Even in the presence of O_2, these mutants exhibit high reversibility with two-state transitions as indicated by the $\Delta_{trs}H_{vH}/\Delta_{trs}H$ ratios (Table 2). A $\Delta_{trs}H_{vH}/\Delta_{trs}H$ ratio equal to unity is evidence of a two-state N $\leftrightarrow$ U transition (*46*).

From the experiments presented in this work, we conclude that oxidation of the metal-coordinating thiolate is the main culprit in inducing irreversibility of the thermal transitions of *P. aeruginosa* azurin. Because of an oxidation reaction between Cu(II) and thiolate, the thermal denaturation of this particular derivative is always irreversible. Removing dissolved O_2 from solutions of both Zn(II)- and Cu(I)-coordinated azurin revealed an inherent thermal reversibility of this β-barrel protein of Greek key topology. Interestingly, there is a difference in the primary mode of inactivation of azurin coordinating Zn(II) and Cu(I). Zn(II) coordination increases the electrophilicity of the sulfur atom of the thiolate, rendering it susceptible to direct nucleophilic attack by molecular oxygen in the denatured state at high temperatures. However, the thermal inactivation of Cu(I)-coordinating azurin appears to occur only via superoxide first produced from a redox reaction between O_2 and Cu(I). Apparently, the latter mode of inactivation is more efficient, and we speculate that Zn(II) azurin should therefore exhibit partial reversibility in the presence of O_2. In addition, removing the oxygen-labile C112 residue gives rise to apoazurin derivatives exhibiting reversible two-state thermal unfolding transitions even in the presence of O_2. The results reported here might apply to irreversible thermal transitions observed in other metalloproteins, especially where the metal is ligated to a cysteine. This would warrant performing DSC measurements under anaerobic conditions to minimize irreversibility and, thus, allow analysis of the transition in terms of a thermodynamic transition model.

ACKNOWLEDGMENT

We thank Hasse Karlsson and Carol Nilsson at Medical Biochemistry, Göteborg University, Sweden, for the mass spectrometric measurements and Ulf Andréasson at the Department of Chemistry, Biochemistry and Biophysics, Göteborg University, Sweden, for the ESR measurements. We also express gratitude to Professor Emeritus Tore Vänngård, also at the Department of Chemistry, Biochemistry and Biophysics, Göteborg University, Sweden, for valuable discussions.

REFERENCES

1. Sanchez-Ruiz, J. M., Lopez-Lacomba, J. L., Cortijo, M., and Mateo, P. L. (1988) *Biochemistry 27*, 1648−1652.
2. Sanchez-Ruiz, J. M. (1992) *Biophys. J. 61*, 921−935.
3. Milardi, D., La Rosa, C., and Grasso, D. (1994) *Biophys. Chem. 52*, 183−189.
4. Lumry, R., and Eyring, H. (1954) *J. Phys. Chem. 58*, 110−120.
5. Engeseth, H. R., and McMillin, D. R. (1986) *Biochemistry 25*, 2448−2455.
6. La Rosa, C., Milardi, D., Grasso, D., Guzzi, R., and Sportelli, L. (1995) *J. Phys. Chem. 99*, 14864−14870.
7. Milardi, D., La Rosa, C., Grasso, D., Guzzi, R., Sportelli, L., and Fini, C. (1998) *Eur. Biophys. J. 27*, 273−282.
8. Guzzi, R., Sportelli, L., La Rosa, C., Milardi, D., Grasso, D., Verbeet, M. Ph., and Canters, G. W. (1999) *Biophys. J. 77*, 1052−1063.
9. Volkin, D. B., Mach, H., and Russel Middaugh, C. (1997) *Mol. Biotechnol. 8*, 105−122.

10. Torchinski, Y. M. (1981) *Sulfur in Proteins*, Pergamon Press, Oxford.
11. Saez, G., Thornalley, P. J., Hill, H. A. O., Hems, R., and Bannister, J. V. (1982) *Biochim. Biophys. Acta 719*, 24−31.
12. Huggins, C., Tapely, D. F., and Jensen, E. V. (1951) *Nature 167*, 592−593.
13. Frensdorff, H. K., Watson, M. T., and Kauzmann, W. (1953) *J. Am. Chem. Soc. 75*, 5157−5166.
14. Zale, S. E., and Klibanov, A. M. (1986) *Biochemistry 25*, 5432−5444.
15. Volkin, D. B., and Klibanov, A. M. (1987) *J. Biol. Chem. 262*, 2945−2950.
16. Tomazic, S. J., and Klibanov, A. M. (1988) *J. Biol. Chem. 263*, 3086−3091.
17. Perry, L. J., and Wetzel, R. (1987) *Protein Eng. 1*, 101−105.
18. Lepock, J. R., Frey, H. E., and Hallewell, R. A. (1990) *J. Biol. Chem. 265*, 21612−21618.
19. McRee, D. E., Redford, S. M., Getzogg, E. D., Lepock, J. R., Hallewell, R. A., and Tainer, J. A. (1990) *J. Biol. Chem. 265*, 14234−14241.
20. Kretschmar, M., and Jaenicke, R. (1999) *J. Mol. Biol. 291*, 1147−1153.
21. Stadtman, E. R. (1993) *Annu. Rev. Biochem. 62*, 797−821.
22. DeBeer, S., Wittung-Stafshede, P., Leckner, J., Karlsson, B. G., Winkler, J. R., Gray, H. B., Malmström, B. G., Solomon, E. I., Hedman, B., and Hodgson, K. O. (2000) *Inorg. Chim. Acta 297*, 278−282.
23. Leckner, J., Wittung, P., Bonander, N., Karlsson, B. G., and Malmström, B. G. (1997) *JBIC, J. Biol. Inorg. Chem. 2*, 368−371.
24. Leckner, L., Bonander, N., Wittung-Stafshede, P., Malmström, B. G., and Karlsson, B. G. (1997) *Biochim. Biophys. Acta 1342*, 19−27.
25. Cavallini, D., De Marco, C., Duprè, S., and Rotilio, G. (1969) *Arch. Biochem. Biophys. 130*, 354−361.
26. Munday, R. (1989) *Free Radical Biol. Med. 7*, 659−673.
27. Gunther, M. R., Hanna, P. M., Mason, R. P., and Cohen, M. S. (1995) *Arch. Biochem. Biophys. 316*, 515−522.
28. Bray, R. C., Cockle, S. A., Fielden, E. M., Roberts, P. B., Rotilio, G., and Calabrese, L. (1974) *Biochem. J. 139*, 43−48.
29. Hodgson, E. K., and Fridovich, I. (1975) *Biochemistry 14*, 5294−5299.
30. Fucci, L., Oliver, C. N., Coon, M. J., and Stadtman, E. R. (1983) *Proc. Natl. Acad. Sci. U.S.A. 80*, 1521−1525.
31. Bonander, N., Leckner, J., Guo, H., Karlsson, B. G., and Sjölin, L. (2000) *Eur. J. Biochem. 267*, 4511−4519.
32. Karlsson, B. G., Pascher, T., Nordling, M., Arvidsson, R. H. A., and Lundberg, L. G. (1989) *FEBS Lett. 246*, 211−217.
33. Pace, N. C., and Scholtz, J. M. (1997) in *Protein Structure. A Practical Approach* (Creighton, T. E., Ed.) pp 299−321.
34. Kirchhoff, W. H. (1993) *Exam: A Two-state Thermodynamic Analysis Program*, NIST Technical Note 1401, 1−103.
35. Guzzi, R., La Rosa, C., Grasso, D., Milardi, D., and Sportelli, L. (1996) *Biophys. Chem. 60*, 29−38.
36. Finazzi-Agrò, A., Rotilio, G., Avigliano, L., Guerrieri, P., Boffi, V., and Mondoví, B. (1970) *Biochemistry 9*, 2009−2014.
37. Falk, K. E., Ivanova, E., Roos, B., and Vänngård, T. (1970) *Inorg. Chem. 9*, 556−562.
38. Peisach, J., and Blumberg, W. E. (1974) *Arch. Biochem. Biophys. 165*, 691−708.
39. Asmus, K.-D. (1984) *Methods Enzymol. 186*, 168−180.
40. Gross, E. L., Draheim, J. E., Curtiss, A. S., Crombie, B., Scheffer, A., Pan, B., Chiang, C., and Lopez, A. (1992) *Arch. Biochem. Biophys. 298*, 413−419.
41. Becktel, W. J., and Baase, W. A. (1987) *Biopolymers 26*, 619−623.
42. Hoitink, C. W. (1993) *Engineering of the Copper Site of Azurin from Alcaligenes denitrificans*, Thesis, Leiden University, The Netherlands.
43. Nar, H., Messerschmidt, A., Huber, R., van de Kamp, M., and Canters, G. W. (1991) *J. Mol. Biol. 221*, 765−772.
44. Nar, H., Huber, R., Messerschmidt, A., Filippou, A. C., Barth, M., Jaquinod, M., van de Kamp, M., and Canters, G. W. (1992) *Eur. J. Biochem. 205*, 1123−1129.
45. Nar, H., Messerschmidt, A., Huber, R., van de Kamp, M., and Canters, G. W. (1992) *FEBS Lett. 306*, 119−124.
46. Privalov, G. P., and Privalov, P. L. (2000) *Methods Enzymol. 323*, 31−62.

BI0157621